Prell, W.L., Wang, P., Blum, P., Rea, D.K., and Clemens, S.C. (Eds.)
Proceedings of the Ocean Drilling Program, Scientific Results Volume 184

17. Alkenone Stratigraphy of the Northern South China Sea for the Past 35 m.y., Sites 1147 and 1148, ODP Leg 184[1]

J.L. Mercer[2, 3] and M. Zhao[2]

ABSTRACT

A reconnaissance study of alkenone stratigraphy for the past 35 m.y. in the northern South China Sea (SCS) using sediments from Sites 1147 and 1148 of Ocean Drilling Program (ODP) Leg 184 has been completed. Alkenones were not detected in sediment samples older than ~31 Ma. However, $C_{37:2}$ appeared in the sedimentary record between ~8 and 31 Ma and both $C_{37:2}$ and $C_{37:3}$ were present between 0 and 8 Ma. These changes in alkenone occurrences may signal a response to global-scale Neogene cooling as well as to monsoon intensification and sea level changes over time as a result of Himalayan uplift and the opening of the SCS. Alternatively, they may be related to an evolutionary record of the development of temperature control on alkenone production in coccolithophores. The $U^{k'}_{37}$ index for 0–8 Ma produces sea-surface temperatures (SST) of 19°–26°C, which are in the range of previously determined glacial–interglacial values for the northern SCS. Before the late Pleistocene (~1.2 Ma), the SST range is between 23° and 26°C with less variation. This change in variability may signify the early stage of intensified winter monsoons where cold wind and waters from the north may not yet have had a significant effect on SST or it may be the evolutionary link between the early development of unsaturated alkenones in coccolithophores and modern temperature control of alkenone production. We believe a long-term alkenone record is useful for further understanding of global-scale neogene cooling, the development of the East Asian monsoon system, and the evolutionary development of tem-

[1]Mercer, J.L., and Zhao, M., 2004. Alkenone stratigraphy of the northern South China Sea for the last 35 m.y., Sites 1147 and 1148, ODP Leg 184. *In* Prell, W.L., Wang, P., Blum, P., Rea, D.K., and Clemens, S.C. (Eds.), *Proc. ODP, Sci. Results,* 184, 1–17 [Online]. Available from World Wide Web: <http://www-odp.tamu.edu/publications/184_SR/VOLUME/CHAPTERS/208.PDF>. [Cited YYYY-MM-DD]
[2]Department of Earth Sciences, Dartmouth College, 6105 Fairchild Science Center, Hanover NH 03755, USA
[3]Department of Atmospheric Science, The University of Wyoming, Department 3038, 1000 East University Avenue, Laramie WY 82071, USA. **mercer@uwyo.edu**

Initial receipt: 10 August 2001
Acceptance: 4 March 2004
Web publication: 2 July 2004
Ms 184SR-208

perature control on alkenone unsaturation. Our data indicate that a high-resolution $U^{k'}_{37}$ record for at least the last ~8 Ma is feasible for the northern SCS.

INTRODUCTION

Among the largest marginal seas, the northern South China Sea's (SCS) climate is greatly affected by the Asian monsoon system (Wang and Wang, 1990; Miao et al., 1994; Shipboard Scientific Party, 2000). In the present regime (Fig. F1), the winter monsoon brings cold winds and water from the north to cool the South China Sea and create a north–south surface temperature gradient (Wyrtki, 1961; Chen et al., 1985; Levitus et al., 1994; Huang et al., 1997a, 1997b). The summer monsoon from the southwest pushes warm air and water into the sea causing warmer and more homogeneous surface temperatures throughout the SCS (Wyrtki, 1961; Chen et al., 1985; Levitus et al., 1994; Huang et al., 1997a, 1997b). The changes of the monsoon system and how it affects the northern SCS during glacial times have been addressed in several studies (Wang and Wang, 1990; Huang et al., 1997a, 1997b; Chen and Huang, 1998; Pelejero et al., 1999a, 1999b). Much lower sea-surface temperatures (SSTs) (by 4°C) and larger seasonality during the last glacial maximum have been attributed to a strengthened winter monsoon, Polar Front shift, and Kurishio Current migration eastward (Huang et al., 1997b; Shipboard Scientific Party, 2000). However, few detailed analyses of the early development of the strengthening of the Asian monsoons have been completed (Shipboard Scientific Party, 2000).

Current models suggest that the Tibetan uplift affected the climates of the Western Pacific marginal seas and China greatly by triggering first the summer monsoon and later the winter monsoon (Liu and Ding, 1982; Wang, 1990, 1997; Shipboard Scientific Party, 2000). The models show an absent monsoon before the uplift (Paleocene and early Eocene) and an unstable monsoon system at the time of the collision between India and Asia (middle Eocene–Oligocene). It is thought that a summer monsoon developed when the initial Himalayan uplift occurred (Miocene–Pliocene), and then both the summer and winter monsoons developed because of intensive uplift during the late Pliocene and into the Pleistocene (Liu and Ding, 1982; Wang, 1990, 1997; Shipboard Scientific Party, 2000). Further, many environmental changes took place on the Asian continent between 8 and 2.6 Ma, including an increase in eolian dust, a shift from C_3 to C_4 plants in Pakistan, and a shift from forested land to grasslands on the Tibetan plateau (Cerling, 1997; Ma et al., 1998; Rea et al., 1998; An et al., 2001). These all imply increased seasonality and have been interpreted as an environmental response to uplift that occurred at 9–8 Ma (An et al., 2001). Even further, An et. al (2001) have identified three periods of monsoon strength variations between 8 and 2.6 Ma using loess-paleosol sequences. At 6–3.6 Ma, the winter and summer monsoon strengths were variable. From 3.6 to 2.6 Ma, winter and summer monsoons were intensified and from 2.6 Ma (the onset of glaciation), there has been an intensified winter monsoon and a weaker summer monsoon (An et al., 2001).

$U^{k'}_{37}$ reconstruction of paleo-SSTs may provide some marine evidence to support the Asian monsoon development models and give us some insight into the environmental response to monsoon development in the northern SCS. The long-chain unsaturated ketones (alkenones),

F1. Modern SST and surface circulation for the SCS, p. 11.

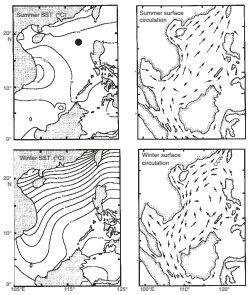

which are produced by Haptophyceae, have been shown to resist biodegradation and diagenesis in marine sediments as old as Eocene (Marlowe et al., 1984; Sun and Wakeham, 1994). The purpose of this study was to reconnoiter a 35-m.y. stratigraphic record of the northern SCS for di- and triunsaturated ketones and evaluate the $U^{k'}_{37}$ record as it is related to the initial strengthening of the monsoon system. Samples from Sites 1147 (18°50.11′N, 116°33.28′E) and 1148 (18°50.17′N, 116°33.94′E) from Ocean Drilling Program (ODP) Leg 184 were used because they provide a long-term sedimentary record of the SCS dating back to ~35 m.y. ago. These sites are situated on the lowermost continental slope off southern China (Fig. F1) and were the most offshore drilling sites during ODP Leg 184 (Shipboard Scientific Party, 2000).

The $U^{k'}_{37}$ method has been applied widely to reconstruct SST. It was originally developed using the di-, tri-, and tetra-unsaturated ketones ($C_{37:2}$, $C_{37:3}$, and $C_{37:4}$), which are produced by Haptophyceae (mostly *Emiliania huxleyi*) in the photic zone (Marlowe et al., 1984; Brassell et al., 1986). Later, it was modified to make use of only the di- and tri-unsaturated ketones, thus called $U^{k'}_{37}$ (Prahl and Wakeham, 1987). The number of double bonds in the alkenones varies between two and four, and as water temperature decreases, unsaturation in the compounds increases (Brassell et al., 1986; Prahl and Wakeham, 1987). The $U^{k'}_{37}$ values were found to be linearly related to temperatures between 8° and 25°C through studies of laboratory-cultured coccolithophores, particulate matter, and core-top sediments (Prahl and Wakeham, 1987; Prahl et al., 1988, 1993; Sikes et al., 1991; Kennedy and Brassell, 1992; Conte et al., 1992; Freeman and Wakeham, 1992; Conte and Eglinton, 1993; Sikes and Volkman, 1993; Rosell-Melé et al., 1995; Madureira et al., 1995; Ternois et al., 1997; Sonzogni et al., 1997). A study by Pelejero and Grimalt (1997) addressed the applicability of the $U^{k'}_{37}$ method in the warm SCS where temperatures range between 23° and 29°C. The relationship between $U^{k'}_{37}$ and temperature was maintained at the upper limits, allowing for application of the $U^{k'}_{37}$ method in warmer ocean waters (Pelejero and Grimalt, 1997). The $U^{k'}_{37}$ method has been applied to the SCS for the past 220 k.y. by Pelejero et al. (1999a, 1999b) where the temperature record followed glacial–interglacial stages. Additionally, high-resolution $U^{k'}_{37}$ records have been completed by Huang et al. for the last 25 k.y. (1997a, 1997b).

METHODS

A total of 116 samples, with a resolution of ~50–100 k.y., were analyzed for long-chain alkenones using gas chromatography (see Huang et al. [1997a] and Pelejero et al. [1999b] for methodology) (Table T1). Sample ages were determined by nannofossil, foraminifer, and paleomagnetic techniques for reference depths (as described in the ODP Leg 184 Preliminary Report) and then interpolated for all depths (Shipboard Scientific Party, 2000). Sediments were freeze-dried and then ground to a fine powder. An internal standard consisting of C_{21}-alcohol, 5α-cholestane, and C_{36} *n*-alkane was added to 1–6 g of sediment, and organic matter was extracted using a Benchmate II robotic station with a mixture of dichloromethane and methanol (3:1 ratio). Briefly, solvent was added by the Benchmate workstation. Samples were manually stirred, sonicated in a water bath for 10 min, and centrifuged at 3000 rpm for 10 min; then the supernatant was drawn off the sediment by the

T1. Results of laboratory analyses, p. 16.

Benchmate workstation. The extraction method was repeated three times, and the supernatants for each sample were combined to ensure complete extraction of alkenones. The supernatant was dried down completely with nitrogen gas and derivatized with *N,O*-bis(trimethylsilyl)trifluoroacetamide. Long-chain alkenones were detected with a Varian 3400 gas chromatograph (GC)/flame ionization detector on an HP-1 crosslinked methylsilicone 50-m column. The initial column temperature was set at 80°C with an increase of 25°C/min to 200°C, then 4°C/min to 250°C, and then 2°C/min to 300°C, where temperature was held constant for 20 min. Alkenones eluted at 300°C (representative peaks are shown in Fig. F2). $U^{k'}_{37}$ values and SST were determined for samples containing both $C_{37:2}$ and $C_{37:3}$ with the following equations (Prahl et al., 1988):

$$U^{k'}_{37} = C_{37:2}/(C_{37:2}+C_{37:3}) \text{ and} \quad (1)$$

$$SST\ (°C) = (U^{k'}_{37} - 0.039)/0.034 \quad (2)$$

In addition, the SSTs from equation 2 were compared to temperatures determined with the following equation, calibrated by Pelejero and Grimalt (1997) for the modern SCS:

$$SST\ (°C) = (U^{k'}_{37} - 0.092)/0.031. \quad (3)$$

Comparison between equations 2 and 3 confirms Pelejero and Grimalt's (1997) conclusions that calibration of the SST equation near the upper boundary gives rise to SST values very close to or within the error limits (~0.5°C, from Villanueva and Gimalt, 1997) of equation 2 (Prahl et al., 1988) (Fig. F3). In this case, the younger samples (<1 Ma) fall within the error limits and the older samples (>1 Ma) fall just outside of the error limits. Here, because of the large temporal scale involved, we express all $U^{k'}_{37}$ values and temperatures using equation 2 (Prahl et al., 1988).

RESULTS/DISCUSSION

Alkenones were not detected in samples older than 31 Ma; only diunsaturated ketones were detected in samples between 8 and 31 Ma, and both di- and triunsaturated ketones were present for the last 8 Ma (Table T1). A statistical analysis of the abundances of $C_{37:2}$ and $C_{37:3}$ as related to age is shown in Figure F4 and clearly suggests three significantly different time periods. Separate categories were used for samples containing both $C_{37:2}$ and $C_{37:3}$ alkenones, samples containing only $C_{37:2}$ alkenones, and samples containing no detectable alkenones.

Samples containing no detectable alkenones had a median age of ~30 Ma with a small range and variance (Fig. F4). It is possible that these samples represent the pre-alkenone conditions in the northern SCS where either coccolithophores had not yet started to produce the compounds (either due to temperatures that were too warm or due to evolutionary processes) and/or migration of the alkenone-producing species into the SCS had not yet occurred (S. Brassell, pers. comm., 2001). It is most likely that the SCS was just too warm during this early time for coccolithophores to produce either of the alkenones. Climate records show a general trend of cooling and increased variability since ~65 Ma,

F2. $C_{37:3}$ and $C_{37:2}$ alkenones, p. 12.

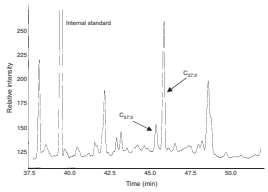

F3. $U^{k'}_{37}$ values and SST, p. 13.

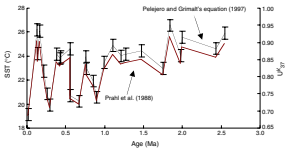

F4. Statistical analysis of alkenones, p. 14.

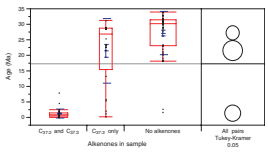

with long periods of steady conditions (Zachos et al., 2001). The Oligocene and early Miocene conditions were comparably "steady," whereas late Miocene records (from ~15 Ma) indicate a globalwide cooling that occurred through the Pliocene (i.e., global-scale Neogene cooling) (Zachos et al., 2001). Further, an alkenone study of the past 4.5 m.y. off the coast of southwest Africa showed steadily high SSTs (>25°C) from ~4.5 to 3.2 Ma and a decreasing trend from ~3.2 to 1 Ma (partial plot in Fig. **F5B**) (Marlow et al., 2000). Similarly, an alkenone study from 2.2 to 6.5 Ma off the northwest coast of Africa showed a cooling trend beginning around 3.2 Ma (Herbert and Schuffert, 1998).

The possibility that the lack of alkenone production was due to evolutionary processes cannot be ruled out. Recent studies have shown that alkenones appear in the sedimentary records first in high latitudes during the early Eocene and later in mid to low latitudes (S. Brassell, pers. comm., 2001). Further, the lack of production may just be due to the lack of alkenone-producing species, as the SCS is believed to have opened at ~32 Ma (Tamaki and Honza, 1991; Briais et al., 1993); thus, this may have been when alkenone-producing coccolithophores were introduced into the SCS. Finally, it is entirely possible that in this environment, these samples are just too old and alkenone concentrations are too low for detection.

Only $C_{37:2}$ was detected in samples from 8 to 31 Ma (Fig. **F4**). With the onset of marine transgression at ~32 Ma, alkenone-producing coccolithophores would have been established in the SCS by the time $C_{37:2}$ occurs in the sediments. There are several possible explanations for the presence of only $C_{37:2}$. If we assume the modern $U^{k'}_{37}$ SST calibration is valid, the first explanation would simply be that warmer SSTs (>28°C) existed and coccolithophores only produced diunsaturated ketones at these points in history. The occurrence of only $C_{37:2}$ is intermittent between ~18 and 23 Ma, which could further indicate an environment that was too warm for the production of alkenones most of the time but, at times, dropped below the required 28°C and allowed for the production of $C_{37:2}$. This could indicate that the SCS was completely free by this time to exchange warm water with the Pacific ocean and/or the summer monsoon system had developed, but a winter monsoon was weak, absent all together, or even fully developed but not detected through alkenone stratigraphy due to average seasonal temperatures >28°C. The second possibility is that the trend shows the evolution of alkenone compounds in coccolithophores. Because it is possible that SST controls on alkenone unsaturation developed as a response to Eocene cooling (S. Brassell, pers. comm., 2001), the large time span with only $C_{37:2}$ present in detectable amounts might be explained as an evolutionary adjustment. Additionally, $C_{37:3}$ compounds may exist in these samples but are undetectable because of very low concentrations and small preferential adsorption of $C_{37:3}$ onto the GC column (Villanueva and Grimalt, 1996). Even if $C_{37:3}$ is present in these samples and is adsorbed onto the GC column, the fact still remains that a $U^{k'}_{37}$ value cannot be determined because the sample consists of virtually only $C_{37:2}$.

$C_{37:2}$ and $C_{37:3}$ were detected in samples younger than 8 Ma (Fig. **F4**). The appearance of $C_{37:3}$ can be used to indicate either the further cooling of the northern SCS or the full evolvement of the temperature control on alkenone production by this time. The SST range for 0–2.5 Ma is between 19° and 26°C. $U^{k'}_{37}$ values and SSTs for these samples are plotted in Figure **F3.** The time resolution for this record is quite low (~50–

F5. Alkenone SST and benthic foraminiferal $\delta^{18}O$ records, p. 15.

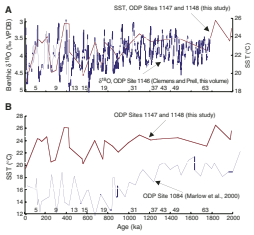

100 k.y. per sample), so only limited interpretations are attempted here. Samples with ages older than 1.2 Ma give SST values of ~24°C with less variation. This is during the early stage of the winter monsoon intensification (An et al., 2001) where cold wind and waters from the north may not yet have had a significant effect on SST. For the last ~1 m.y., the $U^{k'}_{37}$ record shows large variations with a temperature range of 19° to 26°C (Figs. **F3, F5**). Although the lower resolution of the record does not allow us to clearly identify the glacial–interglacial stages within this time span, these temperature ranges are consistent with glacial–interglacial temperature ranges recorded in the northern SCS (Wang and Wang, 1990; Huang et al., 1997a, 1997b; Chen and Huang, 1998; Pelejero et al., 1999a, 1999b). Fluctuations in the SST record also show relatively good agreement with benthic foraminiferal (*Cibicides wuellerstorfi* and *Uvigerina peregrina*) $\delta^{18}O$ values for the past 2 m.y. from Site 1146 during the same ODP leg (Fig. **F5A**) (**Clemens and Prell,** this volume). Comparison of our record with an alkenone SST record from ODP Site 1084 off the southwest coast of Africa (Fig. **F5B**) (Marlow et al., 2000) shows similar SST trends, even though the absolute SSTs are different. Both show an increase in SST oscillations for the last 1 m.y. These marine records are also in agreement with terrestrial indicators of climate change (Cerling et al., 1997; Rea et al., 1998; Ma et al., 1998; An et al., 2001) and support the data that indicate an enhanced winter monsoon since the late stage of Himalayan uplift. Therefore, the most likely explanation for the detection of both types of alkenones is the cooling of the northern SCS because of intensification of the winter monsoon or even broader-scale ocean cooling due to an increase in Northern Hemisphere ice sheets (Shackleton et al., 1984; Raymo, 1994). In addition, sea level drops and the emergence of the islands surrounding the SCS (~6.5 Ma), which would have restricted the exchange of water between the SCS and western Pacific Ocean, could also have enhanced the cooling effect of the winter monsoon (Huang et al., 1997c).

CONCLUSIONS

Multiple interpretations are possible for this long but low-resolution alkenone record. In general, this record provides marine evidence in support of other climate indicators for global-scale Neogene cooling and for the history of monsoon development during the last 35 m.y. This includes vegetation shifts on land (wet to arid) as well as increases in foraminifer abundance due to upwelling and increases in $\delta^{13}C$ and $\delta^{18}O$ values due to a shift toward seasonality (Raymo et al., 1988; Ruddiman and Kutzbach, 1989; Kroon et al., 1991; Cerling, 1997; Ma et al., 1998; Shipboard Scientific Party, 2000). After the collision of India with the Asian continent and during the initial opening of the SCS Basin (before ~31 Ma), alkenones were not detected because of either the lack of production or lack of alkenone-producing species in the SCS. Between ~8 and 31 Ma, only $C_{37:2}$ was detected, which most likely indicates warmer SST (>28°C) or a period of time where temperature control on alkenone unsaturation was evolving. Finally, between 0 and 8 Ma, both $C_{37:2}$ and $C_{37:3}$ were detected, which produces an $U^{k'}_{37}$ index from 0 to 2.5 Ma with SST within the range of previously determined glacial–interglacial values. These results suggest that the $U^{k'}_{37}$ method can serve as a potential long-term glacial–interglacial paleothermometer for the SCS, which can serve as a useful tool for understanding the develop-

ment of the East Asian monsoon system, and that a high-resolution $U^{k'}_{37}$ record for at least the last 8 m.y. may be completed.

ACKNOWLEDGMENTS

This research used samples and/or data provided by the Ocean Drilling Program (ODP). ODP is sponsored by the U.S. National Science Foundation (NSF) and participating countries under management of Joint Oceanographic Institutions (JOI), Inc. This research was partially supported by the Taiwan National Science Council (MZ). We are grateful to Dr. Pinxian Wang and Simon Brassell for discussion and suggestions about the evolution of temperature control on alkenone unsaturation. We'd like to express our appreciation to Dr. Warren Prell and Dr. Timothy Herbert for their constructive and detailed reviews that helped to improve this manuscript.

REFERENCES

An, Z., Kutzbach, J.E., Prell, W.L., and Porter, S.C., 2001. Evolution of Asian monsoons and phased uplift of the Himalaya–Tibetan plateau since late Miocene times. *Nature,* 411:62–66.

Brassell, S.C., Eglinton, G., Marlowe, I.T., Pflaumann, U., and Sarnthein, M., 1986. Molecular stratigraphy: a new tool for climatic assessment. *Nature,* 320:129–133.

Briais, A., Patriat, P., and Tapponnier, P., 1993. Updated interpretation of magnetic anomalies and seafloor spreading stages in the South China Sea: implications for the Tertiary tectonics of Southeast Asia. *J. Geophys. Res.,* 98:6299–6328.

Cerling, T., 1997. Late Cenozoic vegetation change, atmospheric CO_2, and tectonics. *In* Ruddiman, W.F. (Ed.), *Tectonic Uplift and Climate Change:* New York (Plenum), 313–327.

Cerling, T.E., Harris, J.M., MacFadden, B.J., Leakey, M.G., Quade, J., Eisenmann, V., and Ehleringer, J.R., 1997. Global vegetation change through the Miocene/Pliocene boundary. *Nature,* 389:153–158.

Chen, M.T., and Huang, C.-Y., 1998. Ice-volume forcing of winter monsoon climate in the South China Sea. *Paleoceanography,* 13:622–633.

Chen, S., Chen, T., Xu, X., Chen, Z., and Sui, S., 1985. *The Vast South China Sea:* Beijing (China Science Press). (in Chinese)

Conte, M.H., and Eglinton, G., 1993. Alkenones and alkenoate distributions within the euphotic zone of the eastern North Atlantic: correlation with production temperature. *Deep-Sea Res.,* 40:1935–1961.

Conte, M.H., Eglinton, G., and Madureira, L.A.S., 1992. Long-chain alkenones and alkyl alkenoates as palaeotemperature indicators: their production, flux and early sedimentary diagenesis in the eastern North Atlantic. *Org. Geochem.,* 19:287–298.

Freeman, K.H., and Wakeham, S.G., 1992. Variations in the distributions and isotopic compositions of alkenones in Black Sea particles and sediments. *Org. Geochem.,* 19:277–285.

Herbert, T.D., and Schuffert, J.D., 1998. Alkenone unsaturation estimates of late Miocene through late Pliocene sea-surface temperatures at Site 958. *In* Firth, J.V. (Ed.), *Proc. ODP, Sci. Results,* 159T, 17–21 [Online]. Available from World Wide Web: <http://www-odp.tamu.edu/publications/159T_SR/CHAPTERS/CHAP_02.PDF>. [Cited 2004-01-15]

Huang, C.Y., Liew, P.M., Zhao, M., Chang, T.C., Kuo, C.-M., Chen, M.T., Wang, C.H., and Zheng, L.F., 1997a. Deep sea and lake records of the Southeast Asian paleomonsoons for the last 25 thousand years. *Earth Planet. Sci. Lett.,*146:59–72.

Huang, C.Y., Wu, S.F., Zhao, M., Chen, M.T., Wang, C.H., Tu, X., and Yuan, P.B., 1997b. Surface ocean and monsoon climate variability in the South China Sea since the last glaciation. *Mar. Micropaleontol.,* 32:71–94.

Huang, C.-Y., Wu, W.-Y., Chang, C.-P., Tsao, S., Yuan, P.B., Lin, C.-W., and Xia, K.-Y., 1997c. Tectonic evolution of accretionary prism in the arc-continent collision terrane of Taiwan. *Tectonophysics,* 281:31–51.

Kennedy, J.A., and Brassell, S.C., 1992. Molecular records of twentieth century El Niño events in laminated sediments from the Santa Barbara Basin. *Nature,* 357:62–64.

Kroon, D., Steens, T., and Troelstra, S.R., 1991. Onset of monsoonal related upwelling in the western Arabian Sea as revealed by planktonic foraminifers. *In* Prell, W.L., Niitsuma, N., et al., *Proc. ODP, Sci. Results,* 117: College Station, TX (Ocean Drilling Program), 257–263.

Levitus, S., Conkright, M.E., Boyer, T.P., and Burgett, R., 1994. *World Ocean Atlas 1994 and CD-ROM Data Sets:* Washington, D.C. (National Oceanic and Atmospheric Administration).

Liu, T., and Ding, Z., 1982. Pleistocene stratigraphy and Plio/Pleistocene boundary in China. *In* Tung-Sheng, L. (Ed.), *Quaternary Geology and Environment of China:* Beijing (China Ocean Press), 1–9.

Ma, Y.Z., Li, J.J., and Fang, X.M., 1998. Pollen assemblage in 30.6–5.0 Ma redbeds of Linxia region and climate evolution. *Chin. Sci. Bull.,* 43:301–304.

Madureira, L.A.S., Conte, M.H., and Eglinton, G., 1995. Early diagenesis of lipid biomarker compounds in North Atlantic sediments. *Paleoceanography,* 10:627–642.

Marlow, J.R., Lange, C.B., Wefer, G., and Rosell-Melé, A., 2000. Upwelling intensification as part of the Pliocene–Pleistocene climate transition. *Science,* 290:2288–2291.

Marlowe, I.T., Green, J.C., Neal, A.C., Brassell, S.C., Eglinton, G., and Course, P.A., 1984. Long-chain (n-C_{37}–C_{39}) alkenones in the Prymnesiophyceae: distribution of alkenones and other lipids and their taxonomic significance. *Br. Phycol. J.,* 19:203–216.

Miao, Q., Thunell, R.C., and Anderson, D.M., 1994. Glacial–Holocene carbonate dissolution and sea surface temperatures in the South China and Sulu seas. *Paleoceanography,* 9:269–290.

Pelejero, C., and Grimalt, J.O., 1997. The correlation between the U_{37}^k index and sea surface temperature in the warm boundary: the South China Sea. *Geochim. Cosmochim. Acta,* 61:4789–4797.

Pelejero, C., Grimalt, J.O., Heilig, S., Kienast, M., and Wang, L., 1999a. High resolution U^k_{37} temperature reconstructions in the South China Sea over the past 220 kyr. *Paleoceanography,* 14:224–231.

Pelejero, C., Grimalt, J.O., Sarnthein, M., Wang, L., and Flores, J.-A., 1999b. Molecular biomarker record of sea surface temperature and climatic change in the South China Sea during the last 140,000 years. *Mar. Geol.,* 156:109–121.

Prahl, F.G., Collier, R.B., Dymond, J., Lyle, M., and Sparrow, M.A., 1993. A biomarker perspective on prymnesiophyte productivity in the northeast Pacific Ocean. *Deep-Sea Res., Part A,* 40:2061–2076.

Prahl, F.G., Muehlhausen, L.A., and Zahnle, D.L., 1988. Further evaluation of long-chain alkenones as indicators of paleoceanographic conditions. *Geochim. Cosmochim. Acta,* 52:2303–2310.

Prahl, F.G., and Wakeham, S.G., 1987. Calibration of unsaturation patterns in long-chain ketone compositions for paleotemperature assessment. *Nature,* 330:367–369.

Raymo, M.E., 1994. The Himalayas, organic carbon burial, and climate in the Miocene. *Paleoceanography,* 9:399–404.

Raymo, M.E., Ruddiman, W.F., and Froelich, P.N., 1988. Influence of late Cenozoic mountain building on ocean geochemical cycles. *Geology,* 16:649–653.

Rea, D.K., Snoeckx, H., and Joseph, L.H., 1998. Late Cenozoic eolian deposition in the North Pacific: Asian drying, Tibetan uplift, and cooling of the Northern Hemisphere. *Paleoceanography,* 13:215–224.

Rosell-Melé, A., Carter, J.F., Parry, A.T., and Eglinton, G., 1995. Determination of the U^k_{37} index in geological samples. *Anal. Chem.,* 67:1283–1289.

Ruddiman, W.F., and Kutzbach, J.E., 1989. Forcing of late Cenozoic Northern Hemisphere climate by plateau uplift in southern Asia and the American West. *J. Geophys. Res.,* 94:18409–18427.

Sall, J., Lehman, A., and Creighton, L., 2001. *JMP Start Statistics* (2nd ed.): Pacific Grove, CA (Duxbury).

Shackleton, N.J., Blackman, J., Zimmerman, H., Kent, D.V., Hall, M.A., Roberts, D.G., Schnitker, D., Baldauf, J.G., Desprairies, A., Homrighausen, R., Huddlestun, P., Keene, J.B., Kaltenback, A.J., Krumsiek, K.A.O., Morton, A.C., Murray, J.W., and Westberg-Smith, J., 1984. Oxygen isotope calibration of the onset of ice-rafting and history of glaciation in the North Atlantic region. *Nature,* 307:620–623.

Shipboard Scientific Party, 2000. Leg 184 summary: exploring the Asian monsoon through drilling in the South China Sea. *In* Wang, P., Prell, W.L., Blum, P., et al., *Proc. ODP, Init. Repts.,* 184: College Station TX (Ocean Drilling Program), 1–77.

Sikes, E.L., Farrington, J.W., and Keigwin, L.D., 1991. Use of the alkenone unsaturation ratio U^{k}_{37} to determine past sea surface temperatures: core-top SST calibrations and methodology considerations. *Earth Planet. Sci. Lett.,* 104:36–47.

Sikes, E.L., and Volkman, J.K., 1993. Calibration of alkenone unsaturation ratios ($U^{k'}_{37}$) for paleotemperature estimation in cold polar waters. *Geochim. Cosmochim. Acta,* 57:1883–1889.

Sonzogni, C., Bard, E., Rostek, F., Dollfus, D., Rosell-Melé, A., and Eglinton, G., 1997. Temperature and salinity effects on alkenone ratios measured in surface sediments from the Indian Ocean. *Quat. Res.,* 47:344–355.

Sun, M.-Y., and Wakeham, S.G., 1994. Molecular evidence for degradation and preservation of organic matter in the anoxic Black Sea Basin. *Geochim. Cosmochim. Acta,* 58:3395–3406.

Tamaki, K., and Honza, E., 1991. Global tectonics and formation of marginal basins: role of the western Pacific. *Episodes,* 14:224–230.

Ternois, Y., Sicre, M.A., Boireau, A., Conte, M.H., and Eglinton, G., 1997. Evaluation of long-chain alkenones as paleo-temperature indicators in the Mediterranean Sea. *Deep-Sea Res., Part I,* 44:271–286.

Villanueva, J., and Grimalt, J.O., 1996. Pitfalls in the chromatographic determination of the alkenone U^{k}_{37} index for paleotemperature estimation. *J. Chromatogr.,* 723:285–291.

————, 1997. Gas chromatographic tuning of the $U^{k'}_{37}$ paleothermometer. *Anal. Chem.,* 69:3329–3332.

Wang, L., and Wang, P., 1990. Late Quaternary paleoceanography of the South China Sea: glacial/interglacial contrasts in an enclosed basin. *Paleoceanography,* 5:77–90.

Wang, P., 1990. Neogene stratigraphy and paleoenvironments of China. *Palaeogeogr., Palaeoclimatol., Palaeoecol.,* 77:315–334.

————, 1997. Late Cenozoic environment evolution in China: marine factors and records. *Proc. 4th Int. Conf., Evolution of the East Asian Environment,* 264–274.

Wyrtki, K., 1961. *Scientific Results of Marine Investigations of the South China Sea and the Gulf of Thailand: Physical Oceanography of the Southeast Asian Waters:* La Jolla (Univ. of California, Scripps Inst. Oceanography).

Zachos, J., Pagani, M., Sloan, L., Thomas, E., and Billups, K., 2001. Trends, rhythms, and aberrations in global climate 65 Ma to present. *Science,* 292:686–693.

Figure F1. Maps showing the seasonal trends for modern sea-surface temperature (SST) and surface circulation for the South China Sea (after Chen et al., 1985; Levitus et al., 1994; Huang et al., 1997b). The locations of Sites 1147 and 1148 are indicated by the solid circle in the upper left map. CCW = Chinese Coastal Waters.

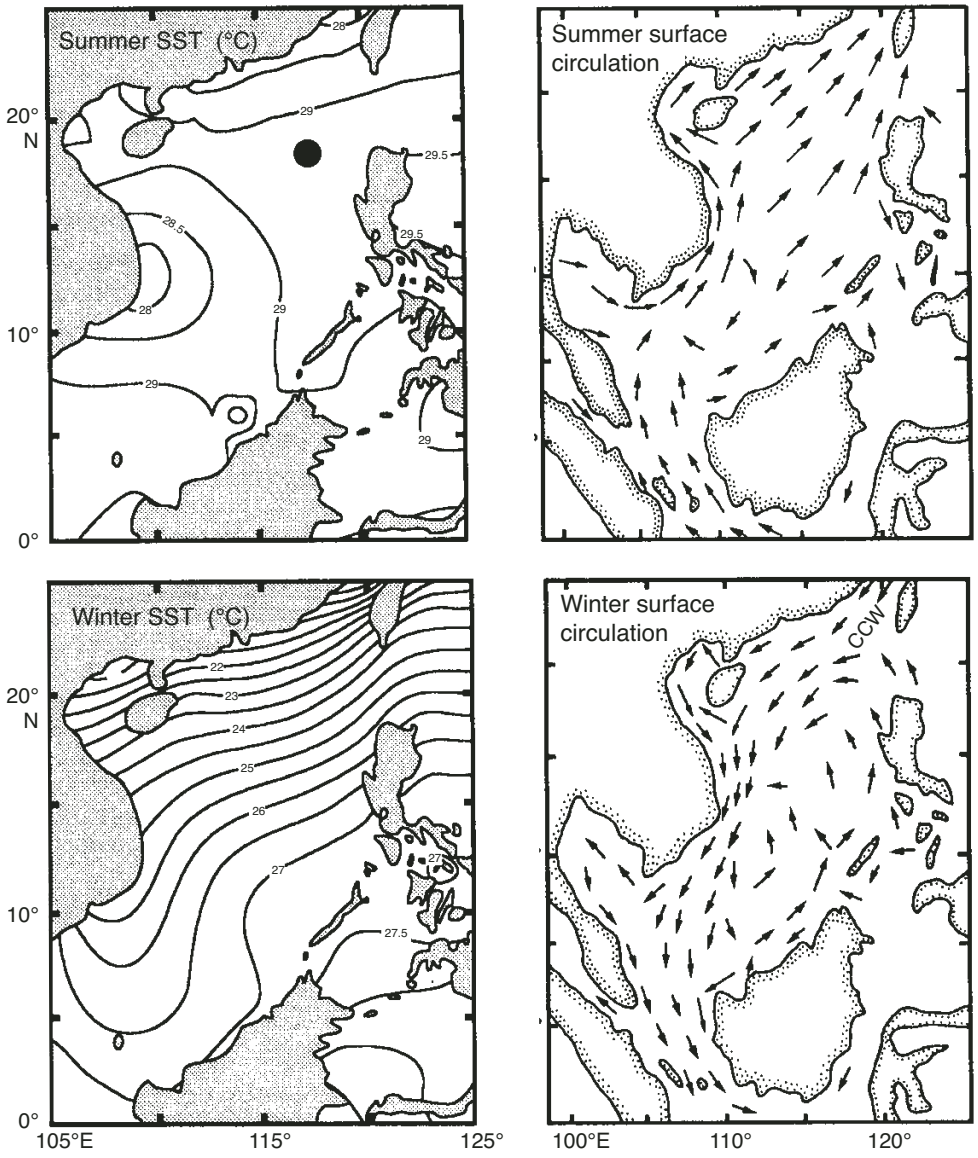

Figure F2. Part of a representative gas chromatogram showing the detection of $C_{37:3}$ and $C_{37:2}$ alkenones for an SCS sample between 0 and 8 Ma.

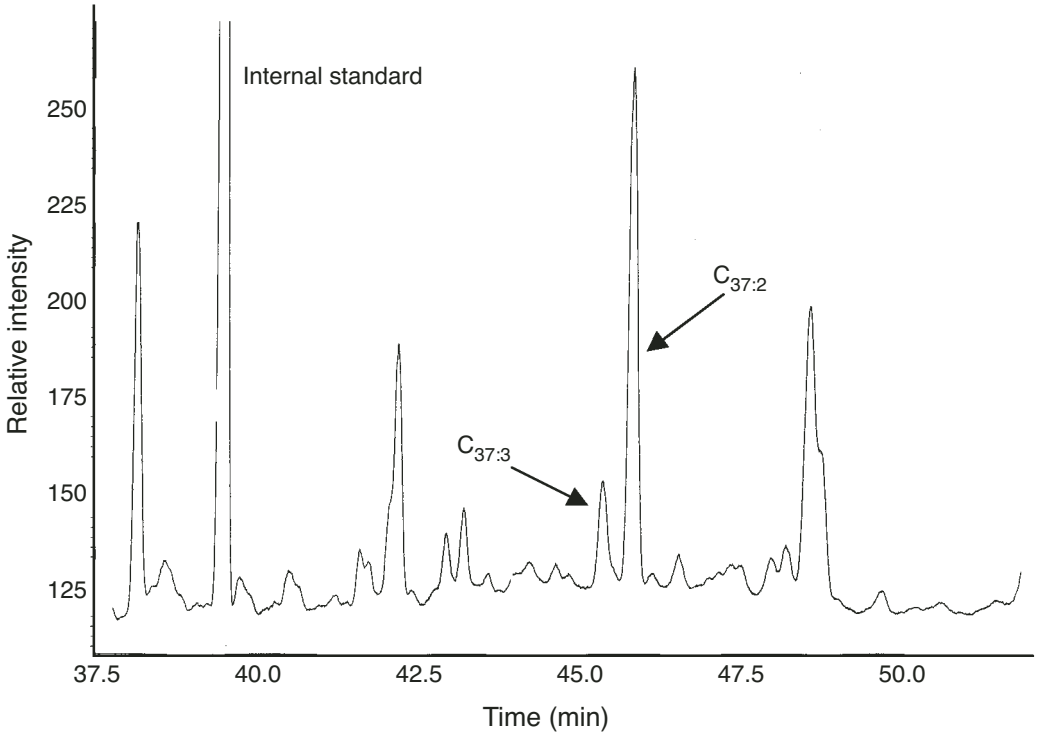

Figure F3. $U^{k'}_{37}$ values and sea-surface temperature (SST) in sediments from Sites 1147 and 1148 are shown for the past ~3 m.y. as the thicker line. Temperatures were calculated using **equation 2** (Prahl et al., 1988). The thin line with error bars represents temperatures calculated using **equation 3** (Pelejero and Grimalt, 1997) for the South China Sea (SCS). For the temperature range in the SCS, the temperature difference between the two equations is almost within the error limits of the indexes.

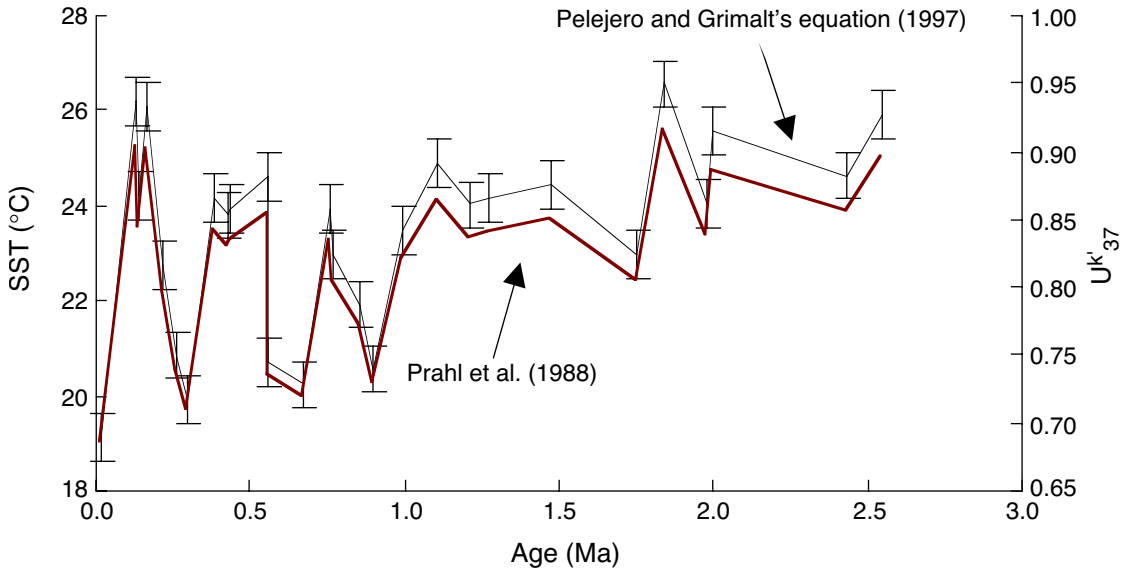

Figure F4. A statistical analysis of alkenones in sediments from Sites 1147 and 1148 for the last 35 m.y. Samples were divided into three categories: $C_{37:2}$ and $C_{37:3}$, $C_{37:2}$ only, and no detectable alkenones. Black dots = individual samples, narrow horizontal bars = means and standard deviations, rectangles = the interquartile range, horizontal bars within the rectangles = median ages. Variance for $C_{37:2}$ and $C_{37:3}$ and no detectable alkenones is quite small, whereas variance for $C_{37:2}$ only spans a wider range. Because the variances are unequal across the groups, a Tukey-Kramer honestly significant difference test for all pairs (the circles on the right) shows that the mean ages for each category are significantly different (Sall et al., 2001).

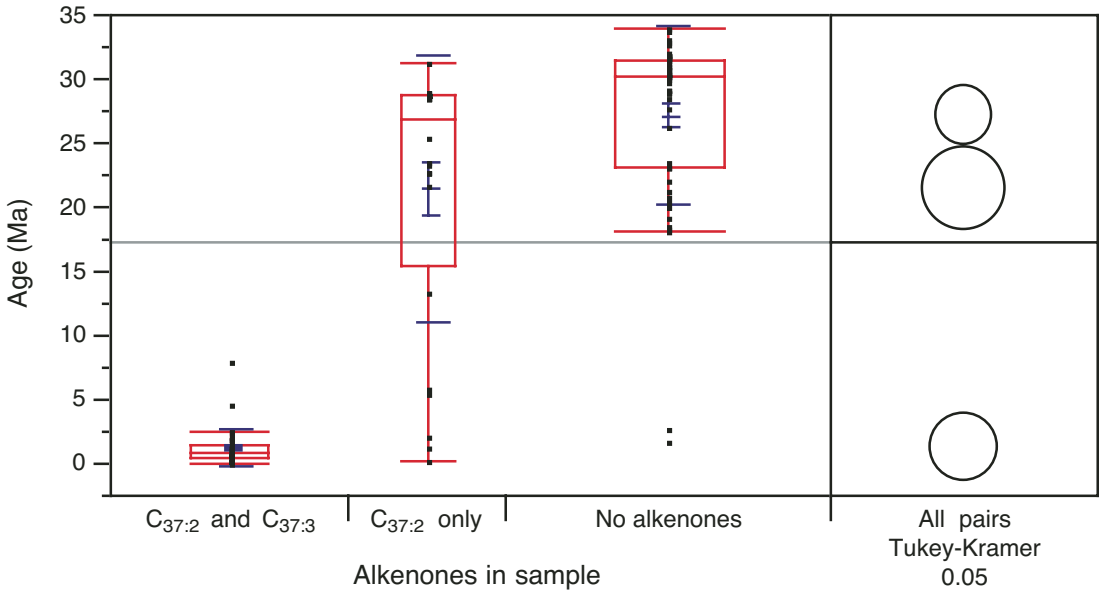

Figure F5. A. Comparison of the alkenone sea-surface temperature (SST) record from Sites 1147 and 1148 for the past 2 m.y. with the benthic foraminiferal (*Cibicides wuellerstorfi* and *Uvigerina peregrina*) $\delta^{18}O$ record for Site 1146 (**Clemens and Prell,** this volume). Increases in temperature generally correspond to lower $\delta^{18}O$ values. **B.** Comparison of the alkenone SST record from Sites 1147 and 1148 with an alkenone SST record from ODP Site 1084 off the southwest coast of Africa (Marlow et al., 2000). Both records show cooling and increased variability starting around 1 Ma. Numbers above the x-axis = selected marine isotope stages (as labeled in **Clemens and Prell,** this volume). VPDB = Vienna Peedee belemnite.

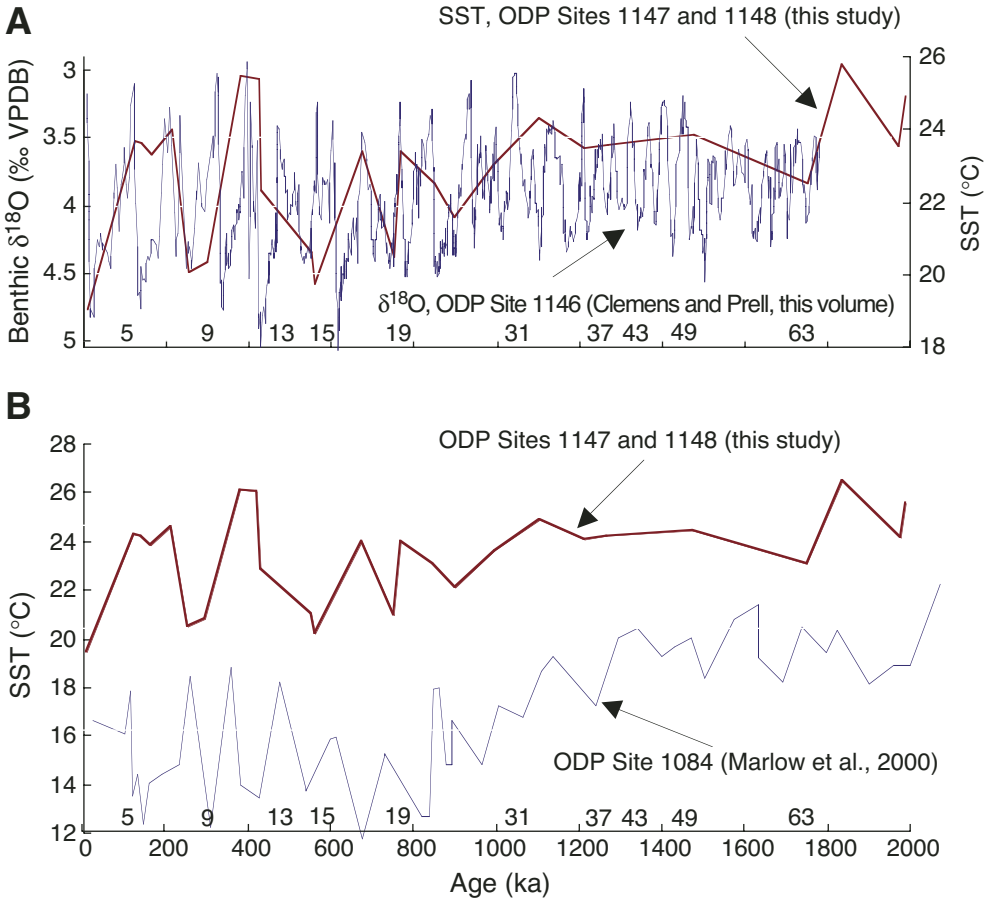

Table T1. Results of laboratory analyses. (See table notes. Continued on next page.)

Sample number	Site	Depth (mcd)	Age (Ma)	Weight (g)	$C_{37:2}$	$C_{37:3}$	$U^{k'}_{37}$	SST (°C)	$C_{37:2}$ (ng/g)	$C_{37:3}$ (ng/g)
	1147									
1		1.225	0.01	0.50	x	x	0.68	19.0	310	142
2		9.425	0.11	1.17						
3		12.425	0.14	1.58	x	x	0.84	23.6	475	88
4		15.425	0.19	1.78	x					
5		22.225	0.28	1.91	x	x	—	—	—	—
6		25.225	0.32	1.59	x	x	—	—	—	—
7		29.925	0.38	1.73	x	x	0.84	23.6	670	126
8		32.925	0.43	1.33	x	x	0.83	23.3	502	103
9		35.925	0.49	2.03	x	x	—	—	—	—
10		39.375	0.56	1.82	x	x	0.85	24.0	121	21
11		45.375	0.68	1.83	x	x	0.72	20.0	—	—
12		63.825	0.90	2.29	x	x	0.73	20.3	—	—
	1148									
13		11.225	0.13	0.66	x	x	0.90	25.4	1645	175
14		14.225	0.17	1.89	x	x	0.90	25.3	—	—
15		17.725	0.22	1.01	x	x	0.80	22.3	1969	503
16		20.725	0.26	1.60	x	x	0.74	20.6	422	150
17		23.725	0.30	1.27	x	x	0.71	19.7	216	89
18		30.225	0.39	1.34						
19		33.225	0.43	1.95	x	x	0.83	23.4	—	—
20		39.725	0.56	1.31	x	x	0.73	20.5	582	210
21		50.175	0.76	1.85	x	x	0.83	23.4	699	140
22		53.175	0.77	2.41	x	x	0.80	22.5	810	197
23		60.775	0.85	2.33	x	x	0.77	21.5	—	—
24		70.745	1.00	2.97	x	x	0.82	23.0	222	49
25		73.745	1.01	3.00	x	x	—	—	—	—
26		77.545	1.11	3.39	x	x	0.86	24.3	382	60
27		83.545	1.17	3.19						
28		90.045	1.19	3.66	x					
29		97.595	1.21	3.25	x	x	0.84	23.5	—	—
30		100.595	1.27	2.55	x	x	0.84	23.6	—	—
31		105.095	1.48	3.96	x	x	0.85	23.8	452	80
32		108.045	1.61	3.50						
33		111.045	1.75	3.62	x	x	0.80	22.5	—	—
34		114.045	1.84	3.02	x	x	0.92	25.8	200	18
35		124.975	1.98	2.58	x	x	0.84	23.5	—	—
36		128.925	1.99	3.91	x	x	0.88	24.9	251	33
37		131.925	2.07	3.82	x	x	—	—	—	—
38		138.875	2.43	3.77	x	x	0.86	24.0	—	—
39		144.875	2.54	3.18	x	x	0.89	25.2	190	22
40		148.595	2.68	3.89	x	x	—	—	—	—
41		151.595	2.79	3.87	x					
42		154.595	2.90	3.50	x					
43		158.095	3.04	3.45	x					
44		161.095	3.17	4.08	x					
45		180.295	4.67	4.27	x	x	—	—	—	—
46		186.895	5.32	3.80	x					
47		199.595	5.85	2.37	x					
48		228.595	7.83	3.67	x					
49		302.525	12.86	3.12						
50		305.395	13.31	5.36						
51		372.715	18.22	2.83						
52		379.285	18.42	4.03						
53		382.265	18.54	3.08						
54		391.995	19.27	2.40						
55		398.685	20.07	2.85						
56		401.805	20.45	2.35						
57		404.815	20.81	2.66						
58		408.295	21.23	3.97						
59		414.295	21.66	8.60	x					
60		423.995	22.08	8.89						
61		437.295	22.66	3.50	x					
62		440.295	22.79	8.74	x					
63		443.295	22.92	8.91	x	x	0.51	14.0	—	—
64		446.995	23.08	4.20						
65		449.995	23.21	4.17						

Table T1 (continued).

Sample number	Site	Depth (mcd)	Age (Ma)	Weight (g)	$C_{37:2}$	$C_{37:3}$	$U^{k'}_{37}$	SST (°C)	$C_{37:2}$ (ng/g)	$C_{37:3}$ (ng/g)
66		452.995	23.34	4.34	x					
67		456.595	23.50	4.36	x					
68		459.595	23.63	4.43						
69		472.195	26.28	6.56						
70		480.235	27.65	4.68						
71		490.525	28.52	3.16	x					
72		495.600	28.56	4.42	x					
73		500.155	28.59	4.19						
74		505.085	28.63	3.60	x					
75		514.835	28.71	3.87	x					
76		519.365	28.75	3.07	x					
77		521.395	28.76	3.55	x					
78		523.785	28.78	6.90	x					
79		527.945	28.81	3.53	x					
80		528.695	28.82	1.70	x					
81		533.630	28.86	7.22						
82		535.250	28.87	3.32						
83		538.380	28.90	3.05	x					
84		543.220	28.94	3.94						
85		570.695	29.15	4.91						
86		583.895	29.26	4.08						
87		609.195	29.69	3.91	x					
88		622.155	30.05	3.30						
89		625.375	30.11	3.59						
90		628.505	30.18	4.30						
91		635.005	30.31	4.66						
92		637.965	30.37	4.71						
93		641.625	30.45	4.25						
94		644.645	30.51	4.43						
95		647.575	30.57	4.08						
96		651.265	30.64	3.63						
97		660.955	30.84	5.27						
98		663.995	30.90	5.27						
99		666.985	30.96	4.65						
100		670.675	31.04	4.21						
101		673.665	31.10	4.57						
102		683.295	31.30	4.18						
103		686.245	31.36	3.92						
104		689.995	31.43	4.49						
105		692.995	31.49	5.29						
106		699.595	31.63	3.69						
107		702.595	31.69	7.19						
108		709.195	31.82	3.98	x					
109		712.195	31.88	4.32						
110		715.195	31.95	4.76						
111		714.635	31.93	5.95						
112		721.295	32.07	5.77						
113		750.125	32.66	3.41						
114		769.125	33.05	4.15						
115		803.280	33.74	4.60						
116		817.805	34.04	2.68						

Notes: SST = sea-surface temperature and is calculated with **equation 2** (Prahl et al., 1988).
x = the compound was detected in that sample. — = not determined.